Centrum voor Wiskunde en Informatica
REPORT*RAPPORT*

Improving Approximate Matrix Factorizations for Implicit Time Integration in Air Pollution Modelling

M.A. Botchev, J.G. Verwer

Modelling, Analysis and Simulation (MAS)

MAS-R0031 December 31, 2000

Report MAS-R0031
ISSN 1386-3703

CWI
P.O. Box 94079
1090 GB Amsterdam
The Netherlands

Improving Approximate Matrix Factorizations for Implicit Time Integration in Air Pollution Modelling

M.A. Botchev

J.G. Verwer
CWI
P.O. Box 94079, 1090 GB Amsterdam, The Netherlands

ABSTRACT
For a long time operator splitting was the only computationally feasible way of implicit time integration in large scale Air Pollution Models. A recently proposed attractive alternative is Rosenbrock schemes combined with Approximate Matrix Factorization (AMF). With AMF, linear systems arising in implicit time stepping are solved approximately in such a way that the overall computational costs per time step are not higher than those of splitting methods. We propose and discuss two new variants of AMF. The first one is aimed at yet a further reduction of costs as compared with conventional AMF. The second variant of AMF provides in certain circumstances a better approximation to the inverse of the linear system matrix than standard AMF and requires the same computational work.

2000 Mathematics Subject Classification: 65M12, 65F30, 65M20, 65M06
1998 ACM Computing Classification System: G.1.8, G.1.3, J.2
Keywords and Phrases: Air pollution modelling, approximate matrix factorization, Rosenbrock methods, large sparse linear systems, stiff ODEs, method of lines
Note: Work carried out under subtheme MAS1.1 "Atmospheric Flow and Transport Problems"

1. Introduction

Typically, in Air Pollution Modelling systems of millions of stiff ODE's, describing advection, vertical mixing (by vertical diffusion and cloud transport) and reactions of the trace gases (or tracers), have to be integrated in time on intervals ranging from months to years [23, 21].

The huge scale of air pollution problems suggests the use of special time integration, e.g. widely used operator splitting, where the physical processes are handled separately. Normally, vertical mixing and reactions are stiff processes and thus require implicit time stepping. On the other hand, the step sizes used for these processes usually lead to CFL numbers below 1 for advection. Therefore, when operator splitting is used, it is natural to apply an explicit scheme for advection and implicit schemes for reactions and vertical mixing. Operator splitting is, however, not always a fortunate choice in the stiff case because the splitting error may spoil the solution. This is especially pronounced for the fast varying trace gases (the so-called radicals) [4, 2, 3, 18].

The most straightforward way to avoid splitting while still treating advection explicitly is to apply an implicit scheme, say a Rosenbrock scheme [5, 8], with a Jacobian containing incomes of only reactions and vertical mixing terms. Another alternative is to use the so-called source splitting [12, 11], where the advection step is performed first and added as the source during the implicit vertical mixing–reaction substep. In both cases Rosenbrock schemes are attractive because they have nice stability properties, often readily allow inexact Jacobians and require a fixed number of linear solves per time step, thus avoiding the Newton iteration process.

The semi-discrete ODE system representing the coupled vertical mixing-reaction process can be written as

$$\dot{\boldsymbol{y}} = \boldsymbol{f}(\boldsymbol{y}), \qquad \boldsymbol{f}(\boldsymbol{y}) = \boldsymbol{V}\boldsymbol{y} + \boldsymbol{r}(\boldsymbol{y}), \qquad y \in \mathbb{R}^N, \quad N = n_z n_t, \tag{1.1}$$

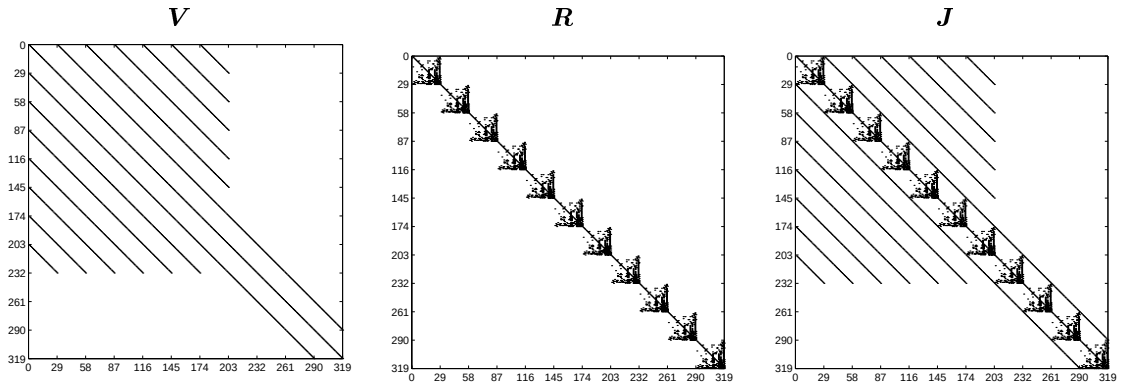

Figure 1: Sparsity structure of the vertical mixing matrix $\boldsymbol{V}$, the reaction Jacobian $\boldsymbol{R}$ and the coupled vertical mixing–reaction Jacobian $\boldsymbol{J} = \boldsymbol{V} + \boldsymbol{R}$ for $n_t = 29$ and $n_z = 11$. The n_z diagonal blocks of $\boldsymbol{R}$ are of size $n_t \times n_t$ and correspond to the chemistry Jacobians per grid point.

where $\boldsymbol{V}$ is the vertical mixing matrix, $\boldsymbol{r}(\boldsymbol{y})$ is the reaction term, n_z is the number of vertical layers and n_t is the number of the trace gases. Typically, $20 \leqslant n_z \leqslant 50$ and $20 \leqslant n_t \leqslant 100$. The linear systems arising in (linearly) implicit schemes applied to (1.1) have the form

$$(\boldsymbol{I} - \tau \boldsymbol{J})\boldsymbol{x} = \boldsymbol{b}, \qquad \boldsymbol{x}, \boldsymbol{b} \in \mathbb{R}^N, \tag{1.2}$$

where $\boldsymbol{J}$ is Jacobian of the reactions and vertical mixing, $\tau = \gamma\,\Delta t$, γ is a parameter of the Rosenbrock scheme, Δt is the step size. In the following we write $\boldsymbol{J} = \boldsymbol{V} + \boldsymbol{R}$ where $\boldsymbol{R}$ is a Jacobian matrix $\partial \boldsymbol{r}(\boldsymbol{y})/\partial \boldsymbol{y}$ evaluated at a certain point.

A serious computational bottleneck is caused by the fact that $\boldsymbol{J}$ usually has a structure that prevents efficient direct solve of (1.2). Matrix $\boldsymbol{I} - \tau \boldsymbol{J}$ is rather large, of size n up to 10^4, and sparse (see Figure 1) but the sparsity would be largely lost during the LU factorization and thus the costs of the factorization as well as of the backsolves would be dramatically increased. Increase of the costs is often simply not feasible, since in Air Pollution Models one has many independent linear systems (1.2) (normally there is one system (1.2) per horizontal grid location, i.e., there are altogether $n_x \times n_y$ systems, where n_x, n_y are horizontal grid sizes).

A natural way to avoid the expensive LU solve for linear systems (1.2) is to settle for an approximate solution. As proposed in [22], for air pollution models this can be done with the help of Approximate Matrix Factorization (AMF),

$$\boldsymbol{I} - \tau \boldsymbol{J} \approx (\boldsymbol{I} - \tau \boldsymbol{R})(\boldsymbol{I} - \tau \boldsymbol{V}), \tag{1.3}$$

by computing $\boldsymbol{x}$ as

$$\boldsymbol{x} := (\boldsymbol{I} - \tau \boldsymbol{V})^{-1}(\boldsymbol{I} - \tau \boldsymbol{R})^{-1}\boldsymbol{b}. \tag{1.4}$$

AMF was introduced in [6, 1]. However, the idea of AMF can already be seen in the ADI method of Peaceman and Rachford. Apart from [22], recent papers on AMF in implicit time integration include [20, 10].

The nice property of AMF is that, when AMF is used within a Rosenbrock scheme applied to the coupled vertical mixing–reactions system, the total computational expenses are just the same as when the Rosenbrock scheme is applied first to vertical mixing and then to reactions within the operator splitting. This was exploited in [22], where a second order L-stable Rosenbrock scheme ROS2 (see

Chapter 9 of [5]) was applied in combination with AMF to different test problems typical for Air Pollution Modelling successfully. The ROS2 scheme can be written as

$$\begin{aligned} &\boldsymbol{y}^{n+1} = \boldsymbol{y}^n + \frac{3}{2}\boldsymbol{k}_1 + \frac{1}{2}\boldsymbol{k}_2, \\ &(\boldsymbol{I} - \gamma\Delta t\boldsymbol{A})\,\boldsymbol{k}_1 = \Delta t\boldsymbol{f}(\boldsymbol{y}^n), \\ &(\boldsymbol{I} - \gamma\Delta t\boldsymbol{A})\,\boldsymbol{k}_2 = \Delta t\boldsymbol{f}(\boldsymbol{y}^n + \boldsymbol{k}_1) - 2\boldsymbol{k}_1. \end{aligned} \tag{1.5}$$

This two-stage method is second order consistent for any matrix $\boldsymbol{A}$. The matrix $\boldsymbol{A}$ is supposed to be an approximation to the Jacobian matrix $\boldsymbol{J} = \boldsymbol{f}'(\boldsymbol{y}_n)$. If the AMF approximation is used, one chooses $\boldsymbol{A}$ such that

$$\boldsymbol{I} - \tau\boldsymbol{A} = (\boldsymbol{I} - \tau\boldsymbol{R})(\boldsymbol{I} - \tau\boldsymbol{V}), \quad \tau = \gamma\Delta t.$$

When using the exact Jacobian, the method has a stability function which is A-stable for $\gamma \geqslant \frac{1}{4}$ and L-stable for $\gamma = 1 \pm \frac{1}{\sqrt{2}}$.

In [4, 3], this ROS2-AMF scheme was also tested against the standard operator Strang splitting in the framework of two real-life air pollution models, the regional LOTOS model [13] and the global TM3 model [19]. The test problems in [4] and [3] were different, e.g., there was no advection in [3] while on the other hand there was no cloud transport in [4]. However, in both situations, within the same amount of computational work, ROS2-AMF gave a better, more accurate solution than operator splitting and source splitting.

In this paper we consider two new modifications of AMF for the coupled vertical mixing–reaction implicit time integration. The first one, AMFe (AMF economical), is aimed at yet a further reduction of costs in AMF with respect to vertical mixing. In AMFe, the LU factorization of $\boldsymbol{I} - \tau\boldsymbol{V}$ is avoided and thus work of order $\mathcal{O}(n_z^3)$ is saved. This can be attractive when the number of vertical layers n_z in the model is relatively large, say more than 30. Another version of AMF, AMF+, is aimed at improving AMF qualitatively. It is shown that in certain cases AMF+ provides significant gain with respect to the standard AMF with no extra costs.

The structure of the paper is as follows. In Section 2 we give more details relevant to the topic, Section 3 introduces AMFe, Section 4 describes AMF+, and the results of numerical tests are discussed in Section 5. The conclusions are drawn in Section 6.

2. Vertical mixing matrix, reaction Jacobian and AMF

For typically used step sizes (≈ 30 min) one has

$$\Delta t\|\boldsymbol{V}\|_2 \sim \mathcal{O}(10), \qquad \Delta t\|\boldsymbol{R}\|_2 \sim \mathcal{O}(10^6), \tag{2.1}$$

whereas smallest in modulus eigenvalues of both of the matrices multiplied with the step size are of order $\mathcal{O}(10^{-5})$. This illustrates the stiffness of the problem and thus the need of (linearly) implicit time integration for the vertical mixing-reaction part.

The sparsity structure of $\boldsymbol{V}$ shown in Figure 1 corresponds to the following ordering of unknowns in the vector $\boldsymbol{x}$ (cf. (1.2)):

$$\begin{aligned} &\boldsymbol{x} = \{x_{km}\}, \qquad k = 1, \ldots, n_z, \quad m = 1, \ldots, n_t, \\ &\boldsymbol{x} = (x_{11}, x_{12}, \ldots, x_{1n_t}, \ \ldots\ , x_{n_z1}, x_{n_z2}, \ldots, x_{n_zn_t}). \end{aligned}$$

With another ordering, namely with

$$\boldsymbol{x} = (x_{11}, x_{21}, \ldots, x_{n_z1}, \ \ldots\ , x_{1n_t}, x_{2n_t}, \ldots, x_{n_zn_t}), \tag{2.2}$$

the matrix $\boldsymbol{V}$ transforms to a block-diagonal matrix with $n_z \times n_z$ dense diagonal blocks V_m, $m = 1, \ldots, n_t$. Each block V_m describes vertical mixing process of the trace gas number m. Often

$$V_m = \text{const}(m), \tag{2.3}$$

i.e. all trace gases are mixed in the same way. In the TM3 model, where the vertical mixing operator also includes the so-called scavenging process, matrices V_m do depend on m. With only vertical diffusion present in the vertical mixing process, matrices V_m would be tridiagonal (it is assumed that the three-point discretization is used). Unlike vertical diffusion, the cloud transport couples vertical layers in the model in a non-local manner thus causing matrices V_m to be dense.

Matrix $-\boldsymbol{V}$ is a (possibly singular) M-matrix[1], it is columnwise weakly diagonally dominant when it is nonsingular and otherwise it has zero column sums. The LU factorization of $\boldsymbol{I}-\tau\boldsymbol{V}$ needed to compute $\boldsymbol{x}$ in (1.4) is done blockwise for each of the blocks $I-\tau V_m$. This costs $\mathcal{O}(n_t n_z^3)$ operations, or $\mathcal{O}(n_z^3)$ operations when all the blocks V_m are identical.

The reaction Jacobian $\boldsymbol{R}$ is a block-diagonal matrix with sparse diagonal blocks R_k, $k=1,\ldots,n_z$, which are reaction Jacobians in a cell k (cf. Fig. 1). The sparsity of the blocks can be efficiently exploited in the course of the LU factorization of $\boldsymbol{I}-\tau\boldsymbol{R}$. Using a special preprocessor tool KPP (Kinetic PreProcessor [17]), an optimal ordering of the trace gases can be found for which the $\boldsymbol{L}$ and $\boldsymbol{U}$ factors are as sparse as possible. In practice this means that the matrix $\boldsymbol{L}+\boldsymbol{U}$ usually has only few percent more fill-in than $\boldsymbol{I}-\tau\boldsymbol{R}$.

Preserving sparsity of the reaction Jacobian is of crucial importance and this, in general, leads to certain limitations in the choice of an efficient approximate solver for (1.2). For example, for the case where cloud transport is absent and thus $\boldsymbol{V}$ is tridiagonal, one could choose for the full LU factorization of $\boldsymbol{I}-\tau\boldsymbol{J}$ performed blockwise. This would however distort sparsity within the blocks, so that the computational work would increase unacceptably.

3. AMFe: economical AMF

Standard AMF (1.3) gives an $\mathcal{O}(\tau^2)$ approximation to $\boldsymbol{I}-\tau\boldsymbol{J}$:

$$(\boldsymbol{I}-\tau\boldsymbol{R})(\boldsymbol{I}-\tau\boldsymbol{V}) = \boldsymbol{I}-\tau\boldsymbol{J}+\tau^2\boldsymbol{R}\boldsymbol{V}. \tag{3.1}$$

A second order approximation can also be achieved with the following more general class of AMF:

$$\begin{aligned} &\boldsymbol{I}-\tau\boldsymbol{J} \approx (\boldsymbol{I}-\tau(\boldsymbol{R}_1+\boldsymbol{V}_1))(\boldsymbol{I}-\tau(\boldsymbol{R}_2+\boldsymbol{V}_2)),\\ &\qquad \boldsymbol{R}=\boldsymbol{R}_1+\boldsymbol{R}_2, \qquad \boldsymbol{V}=\boldsymbol{V}_1+\boldsymbol{V}_2. \end{aligned} \tag{3.2}$$

When the number of vertical layers n_z in the model is large, say more than 30, LU factorization of $n_z\times n_z$ diagonal blocks of $\boldsymbol{I}-\tau\boldsymbol{V}$ can become rather expensive. The LU factorization of $\boldsymbol{I}-\tau\boldsymbol{V}$ can be avoided if one chooses in (3.2)

$$\begin{aligned} &\boldsymbol{R}_1=\boldsymbol{R}, \qquad \boldsymbol{R}_2=0,\\ &\boldsymbol{V}_1=\boldsymbol{V}_L \equiv \text{lower triangular part of } \boldsymbol{V},\\ &\boldsymbol{V}_2=\boldsymbol{V}_U \equiv \text{upper triangular part of } \boldsymbol{V}, \end{aligned}$$

which leads to the following economical AMF (AMFe):

$$\boldsymbol{I}-\tau\boldsymbol{J} \approx (\boldsymbol{I}-\tau(\boldsymbol{V}_L+\boldsymbol{R}))(\boldsymbol{I}-\tau\boldsymbol{V}_U). \tag{3.3}$$

The main diagonals in $\boldsymbol{V}_L$ and $\boldsymbol{V}_U$ are computed in the following way. Each diagonal element in $\boldsymbol{V}_L$ and $\boldsymbol{V}_U$ is first set equal to the sum of the off-diagonal elements of its column taken with the opposite sign. To assure that

$$\mathrm{Diag}(\boldsymbol{V}) = \mathrm{Diag}(\boldsymbol{V}_L)+\mathrm{Diag}(\boldsymbol{V}_U),$$

[1] Matrix A is called an M-matrix if $A=sI-B$ where matrix B is elementwise nonnegative and $s>\rho(B)$, $\rho(B)$ is the spectral radius of B. A is a singular M-matrix if $s=\rho(B)$.

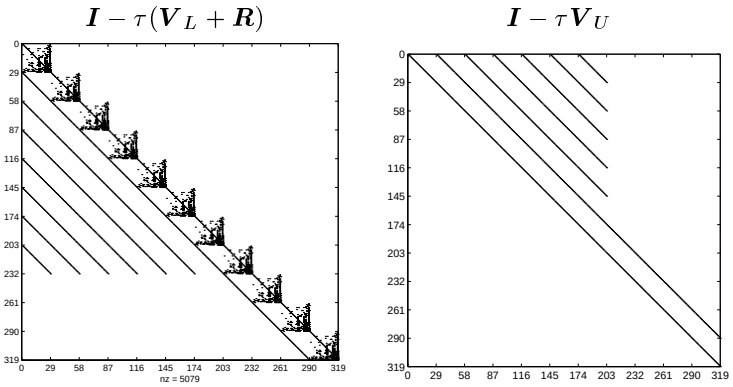

Figure 2: Sparsity structure of the AMFe matrix factors.

Table 1: Computational costs of AMF and AMFe (costs associated with reactions depend on sparsity of $\boldsymbol{R}$ and are not specified).

	Reaction costs	Vertical mixing costs
AMF	n_z LU factorizations of sparse $n_t \times n_t$ blocks, backsolves	n_t LU factorizations of full $n_t \times n_t$ blocks: $\frac{2}{3}n_t n_z^3$ flops backsolves: $n_t n_z(n_z+1)$ flops
AMFe	same as for AMF	backsolves: $n_t n_z^2$ flops

the diagonals are then updated as

$$\begin{aligned} D^+ &:= \mathrm{Diag}(\boldsymbol{V}) - \mathrm{Diag}(\boldsymbol{V}_L) - \mathrm{Diag}(\boldsymbol{V}_U), \\ \mathrm{Diag}(\boldsymbol{V}_L) &:= \mathrm{Diag}(\boldsymbol{V}_L) + \frac{1}{2}D^+, \\ \mathrm{Diag}(\boldsymbol{V}_U) &:= \mathrm{Diag}(\boldsymbol{V}_U) + \frac{1}{2}D^+. \end{aligned} \tag{3.4}$$

Since $-\boldsymbol{V}$ is an M-matrix, with this choice of diagonals matrices $-\boldsymbol{V}_L$ and $-\boldsymbol{V}_U$ are (possibly singular) M-matrices too. As a consequence, matrices $(\boldsymbol{I}-\tau\boldsymbol{V}_L)^{-1}$ and $(\boldsymbol{I}-\tau\boldsymbol{V}_U)^{-1}$ are elementwise nonnegative, just as the matrix $(\boldsymbol{I}-\tau\boldsymbol{V})^{-1}$ is. This property is desirable for preserving positivity.

Sparsity patterns of matrix factors of (3.3) are represented in Figure 2. Both factors can be easily inverted since $\boldsymbol{I}-\tau\boldsymbol{V}_U$ is triangular and $\boldsymbol{I}-\tau(\boldsymbol{V}_L+\boldsymbol{R})$ is block triangular. To invert the diagonal blocks of $\boldsymbol{I}-\tau(\boldsymbol{V}_L+\boldsymbol{R})$, sparse LU factorization is used, in the same way as in the standard AMF for inversion of blocks in $\boldsymbol{I}-\tau\boldsymbol{R}$. In AMFe the costs associated with vertical mixing are significantly reduced (see Table 1).

In fact, with AMFe vertical mixing is handled in an explicit way, so that a Rosenbrock scheme combined with AMFe can be seen as explicit with respect to the vertical mixing. The question arises whether such a scheme will be stable and accurate enough.

Since in AMFe we deal with triangular matrices, to analyze the stability of a Rosenbrock method applied with AMFe we can not consider the usual scalar test equation $\dot{y} = \lambda y$. Analyzing stability of Rosenbrock methods for the more general test case, a *system* of linear ODE's $\dot{y} = Jy$, does not seem an easy task when an approximate Jacobian $A(\approx J)$ is involved. We are able to do this only for the first order Rosenbrock scheme combined with AMFe. Let us consider the following two linear test

systems of n_z ODE's:

$$\dot{y} = Jy, \qquad J = V + D, \quad D = \mathrm{Diag}(\lambda_1, \ldots \lambda_{n_z}), \tag{3.5}$$

$$\dot{y} = Jy, \qquad J = V + \lambda I, \tag{3.6}$$

where $\lambda < 0$, $\lambda_k < 0$ $(k = 1, ..., n_z)$, and V is a symmetric negative semidefinite matrix:

$$V = V^T \leqslant 0.$$

Henceforth, matrix inequalities of the form $A < B$ $(A > B)$ mean that matrix $A - B$ is negative definite (respectively, positive definite) in the real vector space with standard inner product $(x, y) = x^T y$. Note that $A - B$ is not required to be symmetric.

Both test problems (3.5),(3.6) are simplified versions of the vertical mixing-reaction problems as they occur in air pollution models. There are two assumptions under which the reduction to (3.5) is possible. The first one is that the vertical mixing process is described by the same matrix $V_m = V$ for all trace gases m (this can be the case even in full-scale operational models). The second assumption is that the reaction process is linear and the reaction matrix $\boldsymbol{R}$ (cf. Fig. 1) has diagonal blocks with *the same* full set of eigenvectors. Diagonalization of $\boldsymbol{R}$ then would lead us to n_t uncoupled test problems (3.5), one for each trace gas. Under a stronger assumption, that blocks of $\boldsymbol{R}$ are identical, these n_t systems would have the form (3.6). Note that in the latter case $\boldsymbol{RV} = \boldsymbol{VR}$.

The first order Rosenbrock scheme (which we will denote by ROS1) applied to a linear system of ODE's $\dot{y} = Jy$ can be written as

$$y^{n+1} = Sy^n, \qquad S = B^{-1}(B + \tau J), \quad B \approx I - \tau J, \tag{3.7}$$

where $\tau = \Delta t$ is the step size and the approximation B is computed by AMF. Assume that J is symmetric and negative definite. We introduce the so-called "energy" vector and matrix norms as

$$\|y\|_J = \sqrt{(-Jy, y)},$$
$$\|S\|_J^2 = \inf \{M \mid (-JSy, y) \leqslant M(-Jy, y)\}.$$

We use the following result on stability of ROS1 due to Samarskii [15, 16, 7]:
STABILITY CRITERION. *Assume that $J = J^T < 0$ and $B > 0$. Then the scheme (3.7) is stable, i.e.*

$$\|S\|_J \leqslant 1$$

if and only if

$$B + \frac{\tau}{2} J \geqslant 0. \tag{3.8}$$

(Note that B is not required to be symmetric.)

We apply the stability criterion by checking whether (3.8) is true for AMFe, i.e., for B defined as

$$B = (I - \tau(V_L + R))(I - \tau V_U).$$

Since by assumption $V = V^T$, we have $V_L = V_U^T$ (cf. (3.4)) and

$$\begin{aligned} B + \frac{\tau}{2} J &= (I - \tau(V_L + R))(I - \tau V_U) + \frac{\tau}{2} J = \\ &= I - \tau J + \tau^2 (V_L + R) V_U + \frac{\tau}{2} J = \\ &= I - \frac{\tau}{2} J + \tau^2 V_L V_L^T + \tau^2 R V_U. \end{aligned} \tag{3.9}$$

It is clear that the first three terms here are positive semidefinite matrices. We expect the last term to be large because it is second order in τ and R is a stiff matrix. Consider first the case $R = \lambda I$ (test problem (3.6)). We see that $RV_U = \lambda V_U$ is positive semidefinite:

$$(\lambda V_U x, x) = \frac{\lambda}{2}((V_U + V_U^T)x, x) = \frac{\lambda}{2}(Vx, x) \geqslant 0,$$

in other words, condition (3.8) is fulfilled and ROS1-AMFe is stable in this case.

Consider now the case $R = D$ (test problem (3.5)):

$$(DV_U x, x) = \frac{1}{2}((DV_U + V_U^T D)x, x).$$

That the last expression need not be nonnegative for arbitrary negative definite diagonal matrices D can be seen from the following example:

$$\begin{aligned} &V_U = -\begin{bmatrix} 1 & -1 \\ 0 & 1 \end{bmatrix}, \quad V_U + V_U^T = V = -\begin{bmatrix} 2 & -1 \\ -1 & 2 \end{bmatrix}, \quad V = V^T < 0, \\ &D = \begin{bmatrix} -5 & 0 \\ 0 & -1 \end{bmatrix}, \quad DV_U + V_U^T D \text{ has eigenvalues } -0.4031,\ 12.4031\,. \end{aligned} \tag{3.10}$$

However, if the diagonal elements in D do not vary too much, $DV_U + V_U^T D$ will remain positive definite. This is not always but often the case in air pollution models: the diagonal entries λ_k in D can be seen as reaction rates of a given trace gas in the vertical layer k. We can expect that λ_k varies smoothly with k unless, for instance, a cloud darkens layers $1, 2, \ldots, k_0$, switching off photochemical reactions in these layers. The value of λ_{k_0+1} can be then quite different from the value of λ_{k_0} and the scheme can become unstable. After one or two time steps the cloud will disappear from the column and the scheme will get back to the mode with guaranteed stability. Finally, note that (3.8) can be fulfilled eventhough DV_U is not positive semidefinite.

We conclude that ROS1-AMFe can occasionally become unstable (at least in the considered "energy" norm) for a little while, which is not likely to be disastrous. Actually, one can observe the same "instability" effect (that (3.8) may fail to hold when $R = D$) even for the standard AMF (1.3) applied within ROS1. For this ROS1-AMF scheme one would have in (3.9)

$$B + \frac{\tau}{2}J = I - \frac{\tau}{2}J + \tau^2 DV,$$

where DV may not be positive semidefinite.

Because of the explicit nature of AMFe, we expect that the accuracy properties of ROS1-AMFe will be less attractive than those of ROS1-AMF. The poor accuracy properties are often encountered in explicit unconditionally stable schemes, as e.g. in the Du Port-Frankel scheme [14] and in a scheme of Samarskii similar to ROS1-AMFe where the spatially discretized operator is split into lower and upper triangular matrices [16]. However, since the step sizes typically used in air pollution models are not very large with respect to the vertical mixing process (cf. (2.1)), one may hope that the accuracy will not degrade too much. Moreover, one may consider the following way to repair the accuracy of AMFe: if it is known that an active vertical mixing takes place in the layers $k_1, \ldots, k_2$ ($k_1 < k_2$) then we may leave elements of the submatrix of V occupying the $k_1, \ldots, k_2$ rows and columns unsplit in the $\boldsymbol{V}_U$ part. This would lead to the sparsity structure shown in Figure 3.

4. AMF+: IMPROVING AMF

We call AMF+ the following approximation to $\boldsymbol{I} - \tau\boldsymbol{J}$:

$$\boldsymbol{I} - \tau\boldsymbol{J} \approx (\boldsymbol{L}_V - \tau\boldsymbol{R})\boldsymbol{U}_V, \qquad \boldsymbol{L}_V\boldsymbol{U}_V = \boldsymbol{I} - \tau\boldsymbol{V}, \tag{4.1}$$

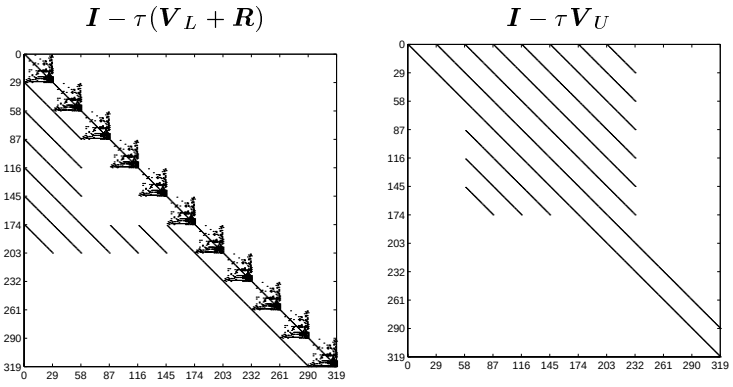

Figure 3: Sparsity structure of the matrix factors in the "repaired" AMFe. $k_1 = 4$ and $k_2 = 6$.

where $\boldsymbol{L}_V$ and $\boldsymbol{U}_V$ are the LU factors of $\boldsymbol{I}-\tau\boldsymbol{V}$ and $\tau = \gamma\Delta t$ (γ is the Rosenbrock scheme parameter). The sparsity portraits of the AMF+ factors $\boldsymbol{L}_V - \tau\boldsymbol{R}$ and $\boldsymbol{U}_V$ coincide with those of the AMFe factors (see Figure 2).

From the relation

$$(\boldsymbol{L}_V - \tau\boldsymbol{R})\boldsymbol{U}_V = \boldsymbol{I} - \tau\boldsymbol{V} - \tau\boldsymbol{R}\boldsymbol{U}_V = \boldsymbol{I} - \tau\boldsymbol{J} + \tau\boldsymbol{R}(\boldsymbol{I} - \boldsymbol{U}_V), \tag{4.2}$$

we see that the error term $\tau\boldsymbol{R}(\boldsymbol{I}-\boldsymbol{U}_V)$ does not seem to be second order in τ. Nevertheless it will be second order if we use the freedom to choose the diagonal elements in one of the LU factors and take

$$\mathrm{Diag}(\boldsymbol{U}_V) = \boldsymbol{I}.$$

The matrix $\boldsymbol{I} - \boldsymbol{U}_V$ is then strictly upper triangular with entries $\mathcal{O}(\tau)$. This can be proven by mathematical induction with respect to the size of the matrix.

If for small τ the AMF+ error term behaves as $\mathcal{O}(\tau^2)$, for large τ it grows at most linearly in τ. This can be seen from the fact that $\boldsymbol{U}_V$ inherits the columnwise diagonal dominance from $\boldsymbol{I} - \tau\boldsymbol{V}$ and therefore

$$\|\boldsymbol{I} - \boldsymbol{U}_V\|_1 < 1,$$

so that

$$\tau\|\boldsymbol{R}(\boldsymbol{I} - \boldsymbol{U}_V)\|_1 \leqslant \tau\|\boldsymbol{R}\|_1\|(\boldsymbol{I} - \boldsymbol{U}_V)\|_1 < \tau\|\boldsymbol{R}\|_1.$$

In fact, $\|\boldsymbol{I} - \boldsymbol{U}_V\|_1$ can be rather small in practice and here lies the main attractiveness of AMF+.

For example, consider the case where the diagonal block V of the matrix $\boldsymbol{V}$, representing vertical mixing of one trace gas (cf. (2.2),(2.3)), is a tridiagonal matrix:

$$I - \tau V = \begin{bmatrix} a_1 & -b_1 & & 0 \\ -b_1 & a_2 & \ddots & \\ & \ddots & \ddots & -b_{n_z-1} \\ 0 & & -b_{n_z-1} & a_{n_z} \end{bmatrix}, \qquad a_k > 0, \quad b_k \geqslant 0, \quad k = 1, \ldots, n_z. \tag{4.3}$$

Since V is either (weakly) diagonally dominant or has zero column sums, we have

$$a_k - b_k - b_{k-1} = \delta_k \geqslant 1, \quad k = 1, \ldots, n_z, \tag{4.4}$$

where it is assumed that $b_0 = b_{n_z} = 0$. It is easy to check that

$$I - \tau V = L_V U_V,$$
$$U_V = \begin{bmatrix} 1 & -u_1 & & 0 \\ 0 & 1 & \ddots & \\ & \ddots & \ddots & -u_{n_z-1} \\ 0 & & 0 & 1 \end{bmatrix}, \qquad u_1 = \frac{b_1}{a_1}, \quad u_k = \frac{b_k}{a_k - b_{k-1}u_{k-1}}, \quad k = 2, \ldots, n_z,$$

and, taking into account (4.4),

$$0 \leqslant u_k = \frac{b_k}{a_k - b_{k-1}u_{k-1}} \leqslant \frac{b_k}{a_k - b_{k-1}} = \frac{b_k}{b_k + \delta_k}. \tag{4.5}$$

We see that u_k can be small if the δ_k are sufficiently large, in other words, if $I - \tau V$ is "sufficiently" diagonally dominant. Estimates on entries of U_V similar to (4.5) can also be obtained for more general situations where $I - \tau V$ is not tridiagonal. Note that similar estimates for the error term of the standard AMF would not be possible (cf. (3.1)).

We analyze stability of ROS1-AMF+ using the test problems (3.5),(3.6) and stability condition (3.8). With

$$B = (L_V - \tau R)U_V, \qquad L_V U_V = I - \tau V,$$

we will check whether the matrix $B + \frac{\tau}{2}J$ is positive definite:

$$B + \frac{\tau}{2}J = L_V U_V - \tau R U_V + \frac{\tau}{2}V + \frac{\tau}{2}R = I - \frac{\tau}{2}V + \frac{\tau}{2}R(I - 2U_V).$$

Since $V = V^T < 0$, the matrix $I - \frac{\tau}{2}V$ is positive definite. Consider the last term, $\frac{\tau}{2}R(I - 2U_V)$. This term can be large because R is a "stiff" reaction matrix. Since R is negative definite, one might hope that $\frac{\tau}{2}R(I - 2U_V)$ is positive definite if $I - 2U_V$ is negative semidefinite. However, it is not negative semidefinite for arbitrary matrices V from the class we are considering (namely, matrices V such that $-V$ is a (singular) Stieltjes matrix[2] with columnwise weak diagonal dominance or zero column sums):

LEMMA 1.

$$\{((I - 2U_V)x, x) \mid (x, x) = 1\} \subset (-3, 1). \tag{4.6}$$

PROOF.

$$((I - 2U_V)x, x) = (x, x) - 2\frac{1}{2}((U_V + U_V^T)x, x) = (x, x) - (\hat{U}x, x),$$

where the matrix $\hat{U} = U_V + U_V^T$ is a symmetric irreducibly diagonally dominant matrix with 2 as main diagonal entries: $\hat{D} = \mathrm{Diag}(\hat{U}) = 2I$. It is easy to check that

$$(x, x) - (\hat{U}x, x) = -(x, x) + 2((I - \hat{D}^{-1}\hat{U})x, x).$$

Since $I - \hat{D}^{-1}\hat{U}$ is the Jacobi iteration matrix of the diagonally dominant matrix $\hat{U}$, its spectral radius is less than one and

$$-2(x, x) \leqslant 2((I - \hat{D}^{-1}\hat{U})x, x) \leqslant 2(x, x),$$

because $I - \hat{D}^{-1}\hat{U}$ is symmetric. □

We can guarantee that $I - 2U_V$ is negative definite for the following class of tridiagonal matrices $I - \tau V$:

[2] Matrix is called a Stieltjes matrix if it is a symmetric M-matrix.

LEMMA 2. *Let $I - \tau V$ be a tridiagonal diagonally dominant matrix given by (4.3),(4.4) and*

$$\delta_k \geqslant b_k, \qquad k = 1, \ldots, n_z - 1. \tag{4.7}$$

Then the matrix $I - 2U_V$ is negative definite.
PROOF. It is easy to check that (4.5) and (4.7) guarantee that

$$u_k \leqslant \frac{1}{2}, \qquad k = 1, \ldots, n_z.$$

Define matrix $\hat{U}$ as in the proof of Lemma 1. Then we have

$$((2U_V - I)x, x) = ((\hat{U} - I)x, x) > 0,$$

because the diagonal entries of $\hat{U}$ are equal to 2 and its off-diagonal entries do not exceed $\frac{1}{2}$, so that the matrix $\hat{U} - I$ is irreducibly diagonally dominant. □

LEMMA 3. *The assumptions of Lemma 2 on $I - \tau V$ are fulfilled if V stems from the standard second order finite difference approximation*

$$[(Ku_z)_z]_k \approx \frac{K_{k+1/2}(u_{k+1} - u_k) - K_{k-1/2}(u_k - u_{k-1})}{h^2}, \qquad K = K(z) > 0,$$

of the diffusion operator $L[u] = (Ku_z)_z$ with Dirichlet boundary conditions.
PROOF. By construction of V. □

As we see, $I - 2U_V$ can be shown to be negative semidefinite for a rather wide class of tridiagonal matrices V. Assume now that $I - 2U_V$ is negative semidefinite. To satisfy the stability condition (3.8) for the ROS1-AMF+ scheme we want $\frac{\tau}{2}R(I - 2U_V)$ to be positive definite. This is true for the case $R = \lambda I$ (test problem (3.5)) and, as discussed earlier (cf. (3.9)), is *likely* to be true if the diagonal elements of $R = D$ (test problem (3.6)) vary smoothly.

Thus we conclude that ROS1-AMF+ can be expected to provide good stability in real-life situations.

5. NUMERICAL EXPERIMENTS

Along with the variants of AMF considered above, one could also use the following alternative factorizations (cf. (1.3),(3.3),(4.1)):

$$\begin{aligned}
\text{standard AMF:} \quad & \boldsymbol{I} - \tau\boldsymbol{J} \approx (\boldsymbol{I} - \tau\boldsymbol{V})(\boldsymbol{I} - \tau\boldsymbol{R}), \\
\text{AMFe:} \quad & \boldsymbol{I} - \tau\boldsymbol{J} \approx (\boldsymbol{I} - \tau\boldsymbol{V}_L)(\boldsymbol{I} - \tau(\boldsymbol{V}_U + \boldsymbol{R})), \\
\text{AMF+:} \quad & \boldsymbol{I} - \tau\boldsymbol{J} \approx \tilde{\boldsymbol{L}}_V(\tilde{\boldsymbol{U}}_V - \tau\boldsymbol{R}), \quad \tilde{\boldsymbol{L}}_V\tilde{\boldsymbol{U}}_V = \boldsymbol{I} - \tau\boldsymbol{V}, \quad \mathrm{Diag}(\tilde{\boldsymbol{L}}_V) = \boldsymbol{I}.
\end{aligned} \tag{5.1}$$

Since the reaction matrix $\boldsymbol{R}$ appears now in the second matrix factor, we will refer to these AMF versions as the R2 versions (indicating that $\boldsymbol{R}$ is in the second factor). Correspondingly, the standard AMF (1.3), AMFe (3.3), and AMF+ (4.1) will be called the R1 versions.

Which version, R1 or R2, is better depends on the problem. However for the standard AMF it is often believed that the R2 version is more accurate since in this case one finishes in (1.4) with a stiff and thus "stable" operator. In our numerical experiments we have tested matrix factorizations in both the R1 and R2 modes.

We consider two linear test problems of the form

$$\begin{aligned}
&\dot{\boldsymbol{y}} = \boldsymbol{J}\boldsymbol{y}, \quad \boldsymbol{J} = \boldsymbol{V} + \boldsymbol{R}, \quad \boldsymbol{y} \in \mathbb{R}^N, \quad N = n_z n_t, \quad n_z = 19,\ n_t = 29, \\
&\boldsymbol{y}(0) = \boldsymbol{y}_0,
\end{aligned} \tag{5.2}$$

where the constant matrices $\boldsymbol{V}$ and $\boldsymbol{R}$ are respectively vertical mixing and reaction Jacobian matrices extracted from the TM3 model [19]. The gas phase chemistry mechanism is described in [9].

The two test problems differ by the choice of $\boldsymbol{V}$. In both cases the matrix $\boldsymbol{V}$ corresponds to a vertical column with an active mixing where scavenging terms were neglected. In the first test, all the trace gases $m = 1, \ldots, n_t$ are mixed in the same way, prescribed by the identical diagonal blocks V_m (see (2.3)).

In the second test, we follow an assumption made in the TM3 model that a number of fast reacting tracers are hardly affected by the vertical mixing process because their reaction rates are much higher than the mixing rate. These tracers are then considered to be immobile which means that in the vertical mixing matrix blocks V_m corresponding to these tracers are set to zero. There are 9 immobile tracers.

For test 2, one can expect that the AMF-based Rosenbrock methods will be more accurate. This is because the AMF error term $\tau^2\|\boldsymbol{RV}\|$ (cf. (3.1)) will be, at least under assumptions leading to the stability test problem (3.6), proportional to $\tau^2|\lambda^{(m)}|\,\|V_m\|$ where $\lambda^{(m)}$ can be seen as the reaction rate of the tracer m. In test 2, for several tracers with large $|\lambda^{(m)}|$ matrices V_m are set to zero, so that the AMF error is reduced. Similar reasoning is valid for AMF+ and AMFe.

The chosen model problems are linear but they are realistic enough to test AMF. In fact, normally in nonlinear atmospheric chemistry problems the local error is occasionally large, mostly due to the day-cycle changes, but since the problem is stiff the errors are damped out fast and do not inflate the global error of AMF-based Rosenbrock schemes (see results in [4, 3]). In our linear problems this unessential temporal increase of the error is absent but the main part of the error (due to the nonstiff components) is still there. Note also that in a nonlinear problem the stiff photochemistry would be switched off during the night whereas our linear problem is constantly stiff.

We test accuracy of the ROS2 scheme (1.5) applied with different AMF's. The accuracy of the different versions is tested against the ROS2 scheme where LU factorization is used to solve the Jacobian systems (1.2) exactly. Thus, we only examine the part of the integration error due to approximate linear solves with AMF's.

We measure accuracy in the following way. Starting with an initial value vector $\boldsymbol{y}_0$ containing realistic mass of the tracers, ten steps with the step size $\Delta t = 20$ min are made. The absolute error vector is then computed as

$$\boldsymbol{e}^n = |\boldsymbol{y}^n - \boldsymbol{y}^n_{\mathrm{AMF}}|,$$

where absolute value of the vector is understood elementwise, n is the time step number, $\boldsymbol{y}^n$ is solution of the "exact" ROS2 scheme and $\boldsymbol{y}^n_{\mathrm{AMF}}$ is the solution of ROS2-AMF scheme (with standard AMF, AMFe, or AMF+). The error vectors $\boldsymbol{e}^n$ are plotted separately for each tracer against the vertical layer number and are compared for different variants of AMF. We prefer to plot the absolute rather than the relative error to see dependence of the error on the vertical layer number. We also check the relative error and when it is unacceptably large we report this explicitly. We say that a certain version of AMF is more accurate than another version of AMF for tracer m if for this tracer the maximum (in all layers) error of the first version is smaller than the maximum error of the second version.

5.1 Testing AMF+

For test 1, both versions of AMF+, namely R1 and R2, clearly outperform the respective versions of AMF (see Figures 4 and 5). We note that, for AMF as well as for AMF+, the R1 versions are significantly more accurate than the R2 versions. For several tracers (e.g. 16, 19, 23) both factorizations produce errors of more than 10%, which is unacceptably large.

AMF+ is more accurate in the R1 mode probably because the matrix $\boldsymbol{U}_V$ in (4.1) is more diagonally dominant than the matrix $\tilde{\boldsymbol{L}}_V$ in (5.1) in the sense that

$$\|\boldsymbol{I} - \boldsymbol{U}_V\|_1 < \|\boldsymbol{I} - \tilde{\boldsymbol{L}}_V\|_1. \tag{5.3}$$

As can be seen from the discussion on accuracy of AMF+ in the previous section, this directly

influences the AMF approximation:

$$\|(\boldsymbol{I}-\tau\boldsymbol{J})-(\text{AMF+ approximation})\|_1 \leqslant \begin{cases}\tau\|(\boldsymbol{I}-\boldsymbol{U}_V)\|_1\|\boldsymbol{R}\|_1 & \text{for the R1 version,}\\ \tau\|(\boldsymbol{I}-\tilde{\boldsymbol{L}}_V)\|_1\|\boldsymbol{R}\|_1 & \text{for the R2 version.}\end{cases}$$

Property (5.3) is quite typical for vertical mixing matrices because, as a consequence of the fact that the mixing is more active in the lower vertical layers, the blocks V_m (see (2.3)) have larger entries in their upper-left corners. Hence, the first columns of the strictly lower triangular part of V_m will be larger in norm than respective columns of the strictly upper triangular part of V_m. This column property is inherited by the LU factors of V_m, thus leading to (5.3).

We observe that performance of the R2 version of AMF+ is quite poor for test 2. However, the R1 version of AMF+ is more accurate than the R1 version of AMF and significantly more accurate than the R2 version of AMF (Figure 6). Comparison of the two versions of AMF is in favor of the R1 version: it is more accurate for 22 tracers. However, except for one tracer, the R2 version of AMF does not lead to unacceptably large errors (as in test 1).

In our discussion in the previous section we argued that AMF+ would gain from the diagonal dominance in $\boldsymbol{V}$. To see whether and to what extent this is true, we have increased the main diagonal in $\boldsymbol{V}$ by a factor 2 and run the same test again. Even in the R2 mode AMF+ outperformed both R1 and R2 versions of AMF (it was more accurate than AMF-R1 and AMF-R2 for 24 and 22 tracers respectively). In the R1 mode AMF+ turned out to be more accurate than both versions of AMF for *all* the tracers. We note that the R2 version of AMF was more accurate than the R1 version of AMF (for 19 trace gases).

5.2 Testing AMFe

Since AMFe is cheaper and, as argued before, presumably less accurate than AMF, we should not expect the AMFe error to be smaller than the AMF error. The aim of the tests is to check to what extent the accuracy is lost with AMFe. Along with AMFe, we have also tested the repaired version of AMFe (see Figure 3) with $k_1 = 2$, $k_2 = 6$.

For test 1, the R2 version of AMFe produces large, often unacceptable errors. However, the errors are typically of the same order of magnitude as the errors of AMF (the R2 version). Moreover, except for one tracer, the errors of AMFe are unacceptably large only when AMF also produces unacceptably large errors.

The results of the R1 versions of AMF and AMFe for test 1 are presented in Figure 7. The errors are much smaller than in the R2 case.

In Figures 8 and 9 the results for test 2 are presented. Again, the R2 modes are less accurate but the loss of accuracy is not significant (the errors are unacceptably large only for one tracer). The errors of AMFe are comparable with the errors of AMF for most of the tracers.

As can be seen from the presented plots, the reparation of AMFe almost always improves its performance significantly.

6. Conclusions

Two new versions of AMF, AMFe and AMF+ were studied analytically and numerically. As was shown, when combined with the ROS1 scheme, both AMF versions provide good stability.

Because of its explicit nature, AMFe was expected to have corrupted accuracy properties. Although this was confirmed in the numerical tests, the errors of AMFe were in most cases of the same order of magnitude as the errors of AMF. When several fast reacting tracers are not transported (test problem 2) these errors are at most several percent, which is acceptable for air pollution models. Taking into account that the accuracy corruption can be repaired as shown, AMFe seems to be an attractive alternative to AMF when the number of vertical layers is large and, therefore, AMF is computationally expensive.

When a higher accuracy is desired, AMF+ is often able to provide this without increase of computational work. AMF+ is also more robust when all the tracers are transported (test problem 1). As

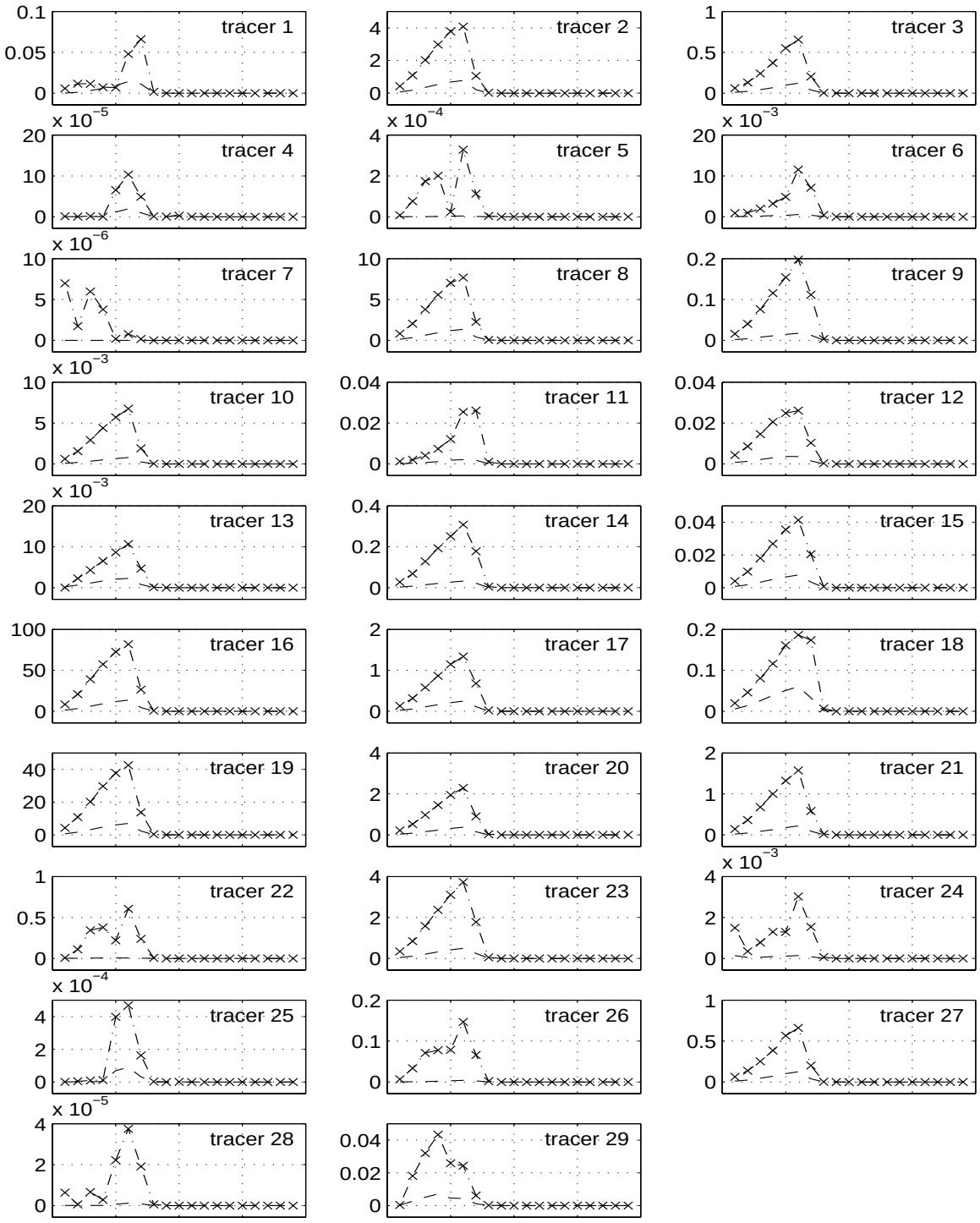

Figure 4: Test 1. Errors of AMF+ (the dashed line) and AMF (the $\times$-line) versus vertical layer number. The ticks on the x-axis correspond to layers 5, 10, 15. Both factorizations are used in the R2 mode, which is unfavorable for AMF+. AMF+ is more accurate for all trace gases.

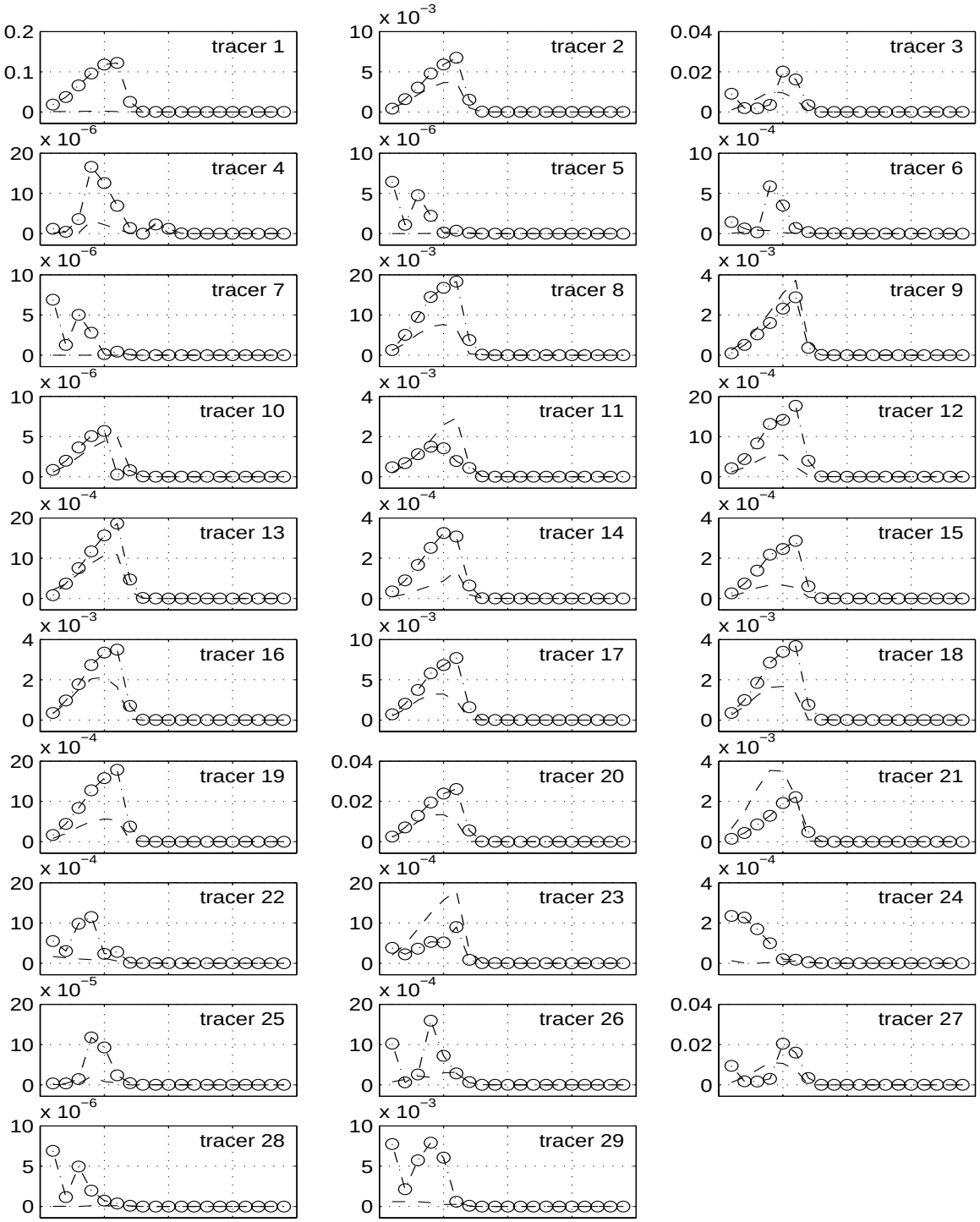

Figure 5: Test 1. Errors of AMF+ (the dashed line) and AMF (the ∘-line) versus vertical layer number. The ticks on the x-axis correspond to layers 5, 10, 15. Both factorizations are used in the R1 mode. AMF+ is more accurate for 25 trace gases.

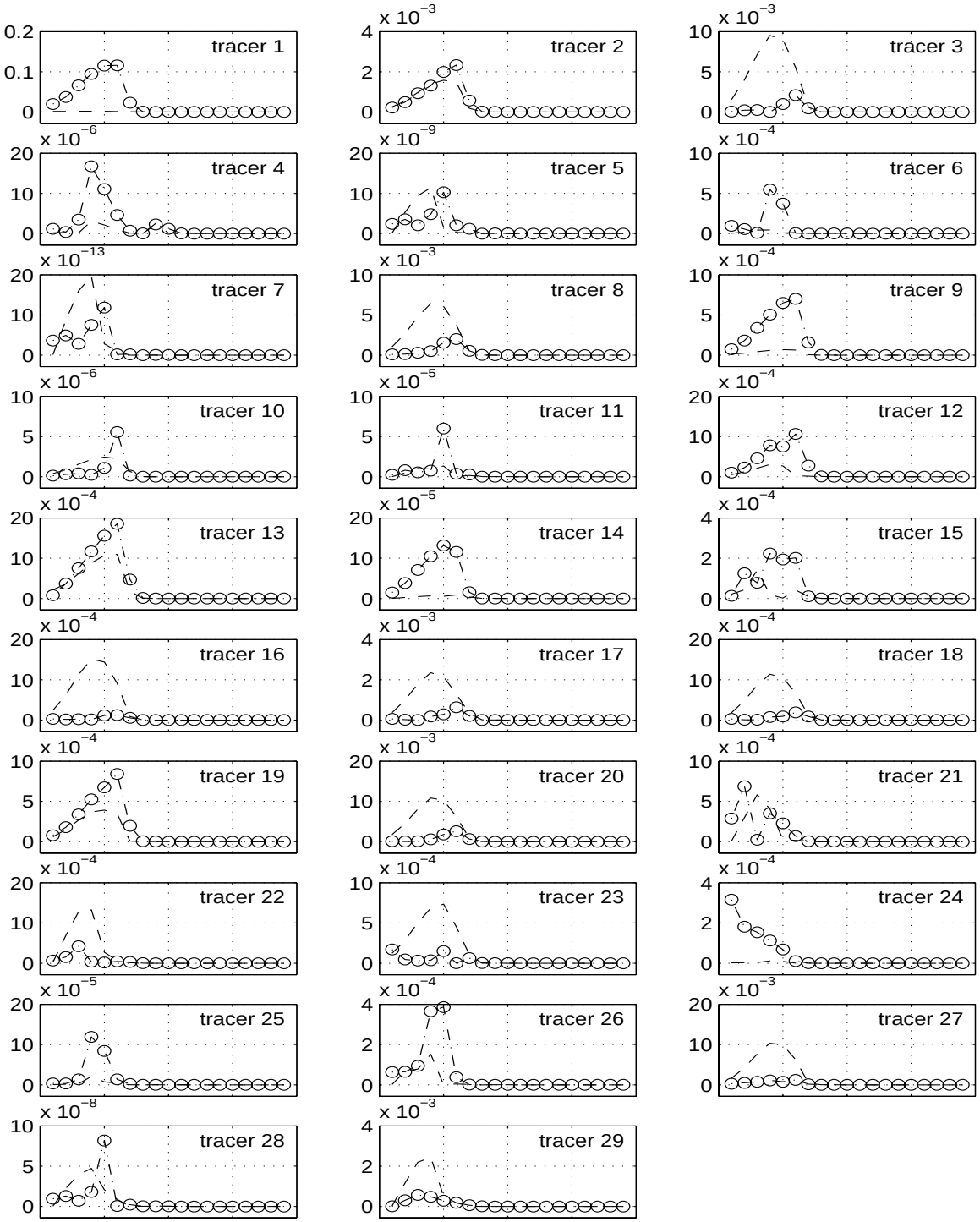

Figure 6: Test 2. Errors of AMF+ (the dashed line) and AMF (the ∘-line) versus vertical layer number. The ticks on the x-axis correspond to layers 5, 10, 15. Both factorizations are used in the R1 mode. AMF+ is more accurate for 17 trace gases.

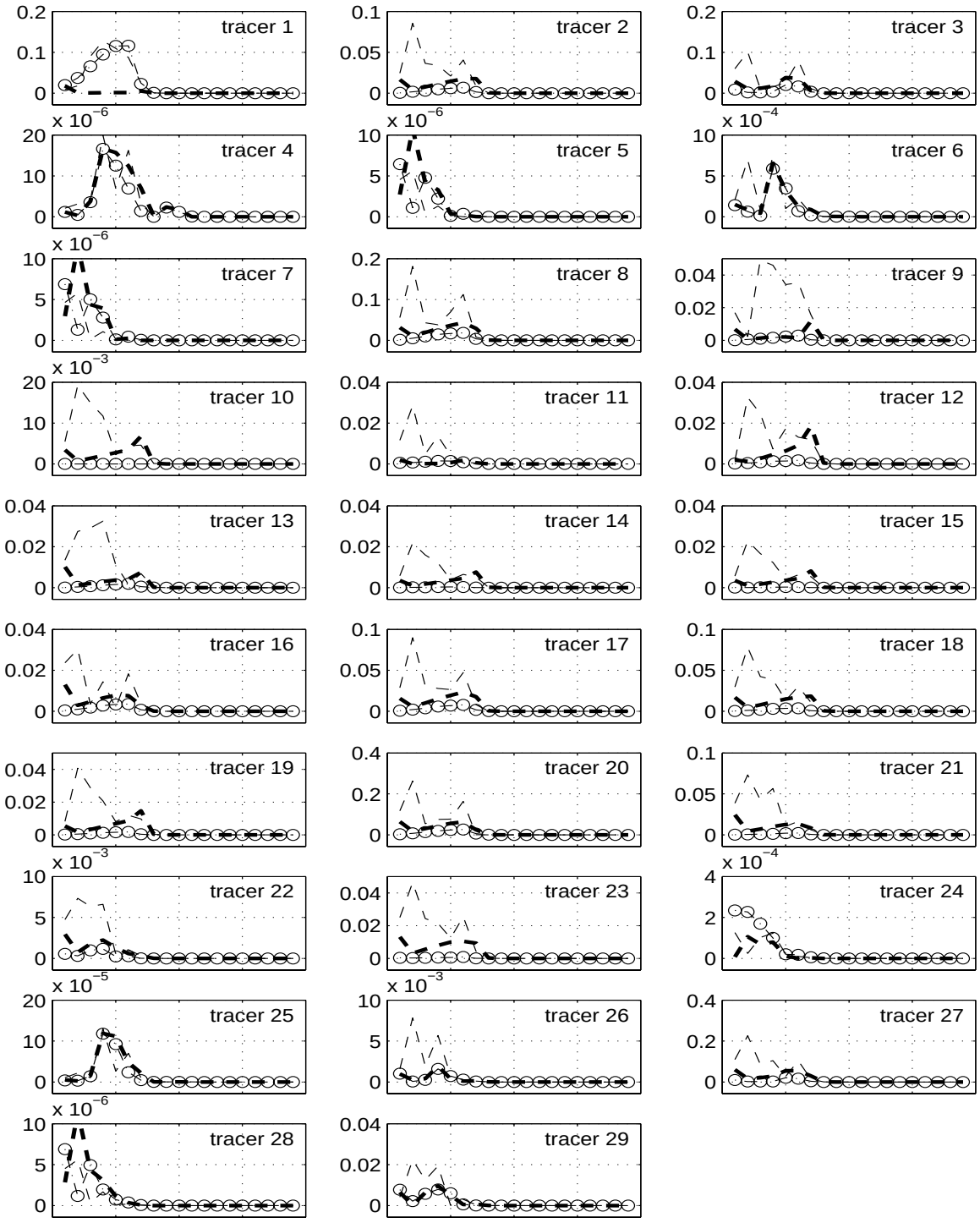

Figure 7: Test 1. Errors of AMF (the ∘-line), AMFe (the dashed line), and the repaired AMFe (the bold dashed line) versus vertical layer number. All factorizations are in the R1 mode. The ticks on the x-axis correspond to layers 5, 10, 15.

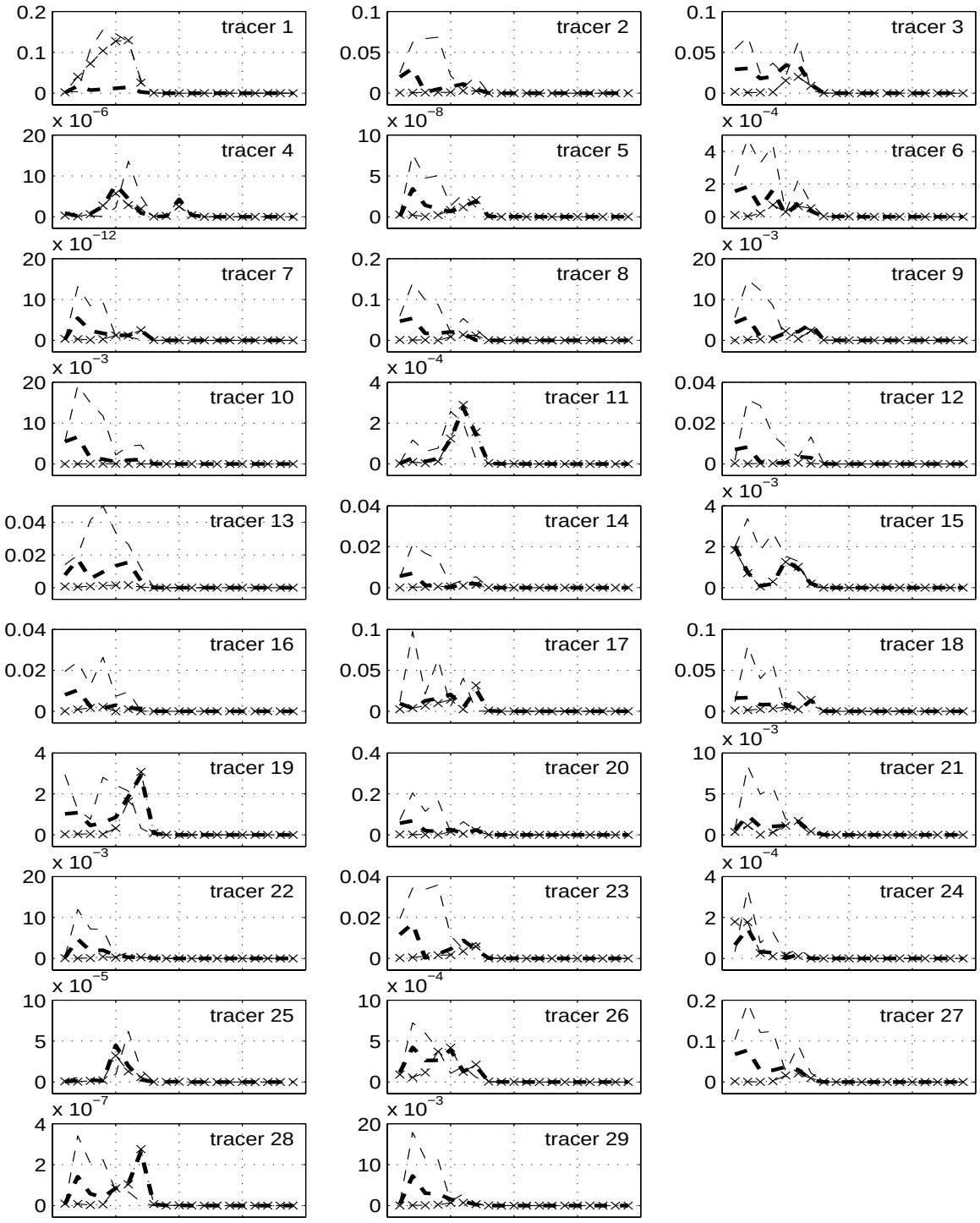

Figure 8: Test 2. Errors of AMF (the $\times$-line), AMFe (the dashed line), and the repaired AMFe (the bold dashed line) versus vertical layer number. All factorizations are in the R2 mode. The ticks on the x-axis correspond to layers 5, 10, 15.

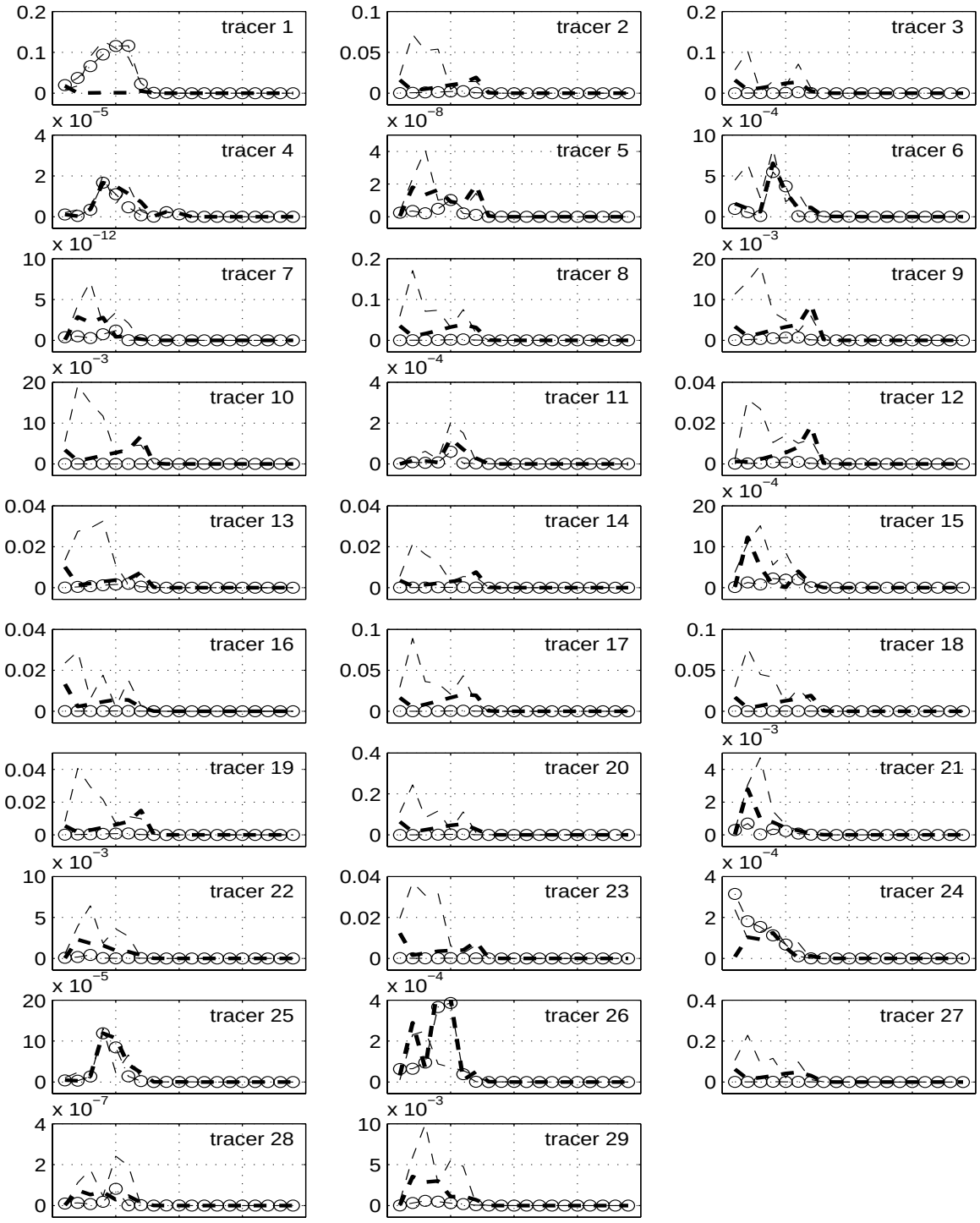

Figure 9: Test 2. Errors of AMF (the ∘-line), AMFe (the dashed line), and the repaired AMFe (the bold dashed line) versus vertical layer number. All factorizations are in the R1 mode. The ticks on the x-axis correspond to layers 5, 10, 15.

shown theoretically and numerically, AMF+ is especially attractive when the vertical mixing matrix is diagonally dominant. We recommend the version of AMF+ where the reaction matrix is kept in the factorization by the first matrix factor, together with matrix $\boldsymbol{L}_V$ (i.e. the R1 version (4.1) rather than the R2 version (5.1)).

Acknowledgements

We thank Patrick Berkvens for his valuable questions and remarks that helped us in the preparation of the paper. We also thank Jos van Dorsselaer and Willem Hundsdorfer for their useful comments concerning performance of Rosenbrock schemes with AMF.

This work has been sponsored by the Netherlands Organization for Scientific Research (NWO) under grant no. 613-302-040.

References

1. R. M. Beam and R. F. Warming. An implicit finite-difference algorithm for hyperbolic systems in conservation-law form. *J. Comput. Phys.*, 22:87–110, 1976.
2. P. J. F. Berkvens, M. A. Botchev, and J. G. Verwer. On the efficient treatment of vertical mixing and chemistry in air pollution modelling. In R. Owens, editor, *CD-ROM Procs. 16th IMACS world congress*, 2000.
3. P. J. F. Berkvens, M. A. Botchev, and J. G. Verwer. Solving vertical transport and chemistry in air pollution models. CWI Report MAS-R0023, 2000. Submitted for publication in Proc. of IMA workshop on "Atmospheric Modeling", March 15-19, 2000.
4. J. G. Blom and J. G. Verwer. A comparison of integration methods for atmospheric transport-chemistry problems. CWI Report MAS-R9910, Amsterdam, 1999. To appear in J. Comp. Appl. Math.
5. K. Dekker and J. G. Verwer. *Stability of Runge-Kutta methods for stiff non-linear differential equations*. North-Holland Elsevier Science Publishers, 1984.
6. E. G. D'yakonov. Difference systems of second order accuracy with a divided operator for parabolic equations without mixed derivatives. *USSR Comput. Math. Math. Phys.*, 4(5):206–216, 1964.
7. S. K. Godunov and V. S. Ryabenkii. *Difference Schemes. An Introduction to the Underlying Theory*. Elsevier Science, 1987.
8. E. Hairer and G. Wanner. *Solving Ordinary Differential Equations II. Stiff and Differential–Algebraic Problems*. Springer Series in Computational Mathematics 14. Springer–Verlag, 1991.
9. S. Houweling, F. J. Dentener, and J. Lelieveld. The impact of non-methane hydrocarbon compounds on troposhperic photochemistry. *J. Geophys. Res.*, 103(10):673–696, 1998.
10. W. Hundsdorfer. Accuracy and stability of splitting with stabilizing corrections. CWI Report MAS-R9935, Amsterdam, 1999.
11. C. Kessler. *Entwicklung eines effizienten Lösungverfahrens zur modellmässigen Beschreibung der Ausbreitung und chemischen Umwandlung reaktiver Luftschadstoffe*. PhD thesis, Facultät für Maschinenbau der Universtät Karlsruhe, Aachen, 1995.
12. O. Knoth and R. Wolke. A comparison of fast chemical kinetic solvers in a simple vertical diffusion model. In S.-V. Gryning and M. Millán, editors, *Air Pollution Modelling and Its Application X*, pages 287–294, New York, 1994. Plenum Press.

13. http://www.cwi.nl/~gollum/lotos/, LOTOS: LOng Term Ozone Simulation. CWI, Amsterdam.
14. R. D. Richtmyer and K. W. Morton. *Difference methods for initial-value problems.* Interscience Publishers John Wiley & Sons, Inc., New York-London-Sydney, 1967. Second edition. Interscience Tracts in Pure and Applied Mathematics, No. 4.
15. A. A. Samarskii. Regularization of difference schemes. *USSR Comput. Math. and Math. Phys.*, 7:62–93, 1967.
16. A. A. Samarskii. *Theorie der Differenzenverfahren.* Akademische Verlagsgesellschaft Geest & Portig K.-G., Leipzig, 1984. Translated from the Russian by Gisbert Stoyan.
17. A. Sandu, F. A. Potra, G. R. Carmichael, and V. Damian. Efficient implementation of fully implicit methods for atmospheric chemical kinetics. *J. Comput. Phys.*, 129:101–110, 1996.
18. B. Sportisse. An analysis of operator splitting techniques in the stiff case. *J. Comput. Phys.*, 161(1):140–168, 2000.
19. http://www.phys.uu.nl/~peters/TM3/TM3S.html, the TM3 model homepage. Utrecht University, Utrecht.
20. P. van der Houwen and B. P. Sommeijer. Approximate factorization for time-dependent partial differential equations. CWI Report MAS-R9915, Amsterdam, 1999. To appear in J. Comput. Appl. Math. (2000).
21. J. G. Verwer, W. Hundsdorfer, and J. G. Blom. Numerical time integration for air pollution models. CWI Report MAS-R9825, Amsterdam, 1998. To appear in "Surveys for Mathematics in Industry".
22. J. G. Verwer, E. J. Spee, J. G. Blom, and W. Hundsdorfer. A second order Rosenbrock method applied to photochemical dispersion problems. *SIAM J. Sci. Comput.*, 20:456–480, 1999.
23. Z. Zlatev. *Computer treatment of large air pollution models.* Kluwer Academic Publishers, 1995.